Effects of Combustion-Induced Vortex Breakdown on Flashback Limits of Syngas-Fueled Gas Turbine Combustors

Final Technical Report

Reporting Period Start Date: 04/01/08

Reporting Period End Date: 04/30/11

Principal Author

Ahsan Choudhuri, PhD

July 2011

Department of Energy Grant DE-FG26-08NT0001719

Center for Space Exploration and Technology Research
Mechanical Engineering Department
500 W. University Ave.
The University of Texas El Paso
El Paso, TX 79968

Disclaimer

This report was prepared as an account of work sponsored by an agency of the United States Government. Neither the United States Government nor any agency thereof, nor any of their employees, makes any warranty, express or implied, or assumes any legal liability or responsibility for the accuracy, completeness, or usefulness of any information, apparatus, product, or process disclosed, or represents that its use would not infringe privately owned rights. Reference herein to any specific commercial product, process, or service by trade name, trademark, manufacturer, or otherwise does not necessarily constitute or imply its endorsement, recommendation, or favoring by the United States Government or any agency thereof. The views and opinions of authors expressed herein do not necessarily state or reflect those of the United States Government or any agency thereof.

Abstract

Turbine combustors of advanced power systems have goals to achieve very low pollutants emissions, fuel variability, and fuel flexibility. Future generation gas turbine combustors should tolerate fuel compositions ranging from natural gas to a broad range of syngas without sacrificing operational advantages and low emission characteristics. Additionally, current designs of advanced turbine combustors use various degrees of swirl and lean premixing for stabilizing flames and controlling high temperature NO_x formation zones. However, issues of fuel variability and NO_x control through premixing also bring a number of concerns, especially combustor flashback and flame blowout.

Flashback is a combustion condition at which the flame propagates upstream against the gas stream into the burner tube. Flashback is a critical issue for premixed combustor designs, because it not only causes serious hardware damages but also increases pollutant emissions. In swirl stabilized lean premixed turbine combustors onset of flashback may occur due to (i) boundary layer flame propagation (critical velocity gradient), (ii) turbulent flame propagation in core flow, (iii) combustion instabilities, and (iv) upstream flame propagation induced by combustion induced vortex breakdown (CIVB).

Flashback due to first two foregoing mechanisms is a topic of classical interest and has been studied extensively. Generally, analytical theories and experimental determinations of laminar and turbulent burning velocities model these mechanisms with sufficient precision for design usages. However, the swirling flow complicates the flashback processes in premixed combustions and the first two mechanisms inadequately describe the flashback propensity of most practical combustor designs.

The presence of hydrogen in syngas significantly increases the potential for flashback. Due to high laminar burning velocity and low lean flammability limit, hydrogen tends to shift the combustor operating conditions towards flashback regime. Even a small amount of hydrogen in a fuel blend triggers the onset of flashback by altering the kinetics and thermophysical characteristics of the mixture. Additionally, the presence of hydrogen in the fuel mixture modifies the response of the flame to the global effects of stretch and preferential diffusion.

Despite its immense importance in fuel flexible combustor design, little is known about the magnitude of fuel effects on CIVB induced flashback mechanism. Hence, this project investigates the effects of syngas compositions on flashback resulting from combustion induced vortex breakdown. The project uses controlled experiments and parametric modeling to understand the velocity field and flame interaction leading to CIVB driven flashback.

Table of Contents

Executive Summary

This initial portion of this report presents experimental measurements of the critical velocity gradient and flashback behavior of H_2-CO and H_2-CH_4 mixtures. Effects of H_2 concentration on the flashback behavior of flames of these fuel mixtures are discussed. For H_2 concentration burner and scaling studies the critical velocity gradient (g_F), defined as the ratio of the square of the laminar burning velocity to the thermal diffusivity of the mixture ($\mathbf{g_F = c\frac{S_L^2}{\alpha}}$), was used to quantify the flashback propensity of the flames. The critical velocity gradient of both H_2-CH_4 and H_2-CO flames changed nonlinearly with the increase in H_2 contents in the mixture. The critical velocity gradient (g_F) of 5%-95% and 15%-85% H_2-CO mixtures somewhat agreed with the scaling relation and yielded an average c value of 0.04. Similarly, values of a 25%H_2-75%CH_4 for different burner diameters were also fitted using the scaling relation yielding an average c value of 0.044. The g_F values of 25%-75% H_2-CO mixture showed nonlinear variation with the S_L^2/α ratio (especially for $S_L^2/\alpha > 19{,}000\ s^{-1}$), and at a lower S_L^2/α ratios burner diameter had small effect on critical velocity gradient measurements. The opposite trend was observed for a 25%-75% H_2-CH_4 mixture showing non-linear variation at a lower S_L^2/α ratios (for $S_L^2/\alpha > 5{,}600\ s^{-1}$) and having less affect at higher S_L^2/α ratios.

For the second part of the report the results from a study of flame flashback attributed to combustion induced vortex breakdown (CIVB) is presented for flames yielded from hydrogen (H_2) - carbon monoxide (CO) fuel blends and actual synthesized gas (syngas) mixtures. A two-fold experimental approach, consisting of a high definition digital imaging system and a high speed PIV system, was employed. The main emphasis was on the effect of concentration of different constituents in fuel mixtures on flashback limit. In addition, the effect of Swirl Number on flashback propensity was discussed. The percentage of H_2 in fuel mixtures played the dominant role when CIVB flashback occurred. For a given air mass flow rate, the mixture containing a higher percentage of H_2 underwent flashback at much leaner conditions. Flashback maps for actual syngas fuel compositions showed a distinct behavior when various concentrations of diluents were introduced in the mixture. For the two major diluents tested, carbon dioxide (CO_2) and nitrogen dioxide (NO_2), CO_2 was more dominant. The effect of swirl number on the flashback propensity was also tested and showed a decrease with an increase in Swirl Number. This section also provides an analysis of flow field of reacting flames which revealed complex vortex-chemistry interactions leading to vortex breakdown and flashback. Based on the experimental results a parametric model similar to Peclet Number approach was developed employing a flame quenching concept. A value of the quench parameter, C_{quench} was obtained from the correlation of flow Peclet Number and flame Peclet Number, which was observed to be dominated by the fuel composition rather than Swirl Number.

The third section of this report investigates the modeling of flashback phenomena in a gas turbine combustor. The current work presents some preliminary results using LES to simulate the flashback phenomena for methane and syngas fuels using both commercial code (CHEMKIN CFD) and open source codes (OpenFOAM). An LES model is developed for both isothermal and reacting flow in a laboratory scale gas turbine combustor. Future work seeks to validate the isothermal model against experimental data obtained from the high speed Particle Image Velocimetry (PIV).

Project Information

Project Title: Effects of Combustion-Induced Vortex Breakdown of Flashback Limits of Syngas-Fueled Gas Turbine Combustors

Grant No: DE-FG26-08NT0001719

Agency: National Energy Technology Laboratory, Department of Energy

DOE Project Manager:
Norm Popkie
Project Manager
National Energy Technology Laboratory
3610 Collins Ferry Road, P.O. Box 880
Morgantown, WV. 26507-0880
Phone: (304) 285-0977
Email: norman.popkie@netl.doe.gov

Project Period: 04/01/08-04/30/11

Principal Investigator:
Ahsan R. Choudhuri, PhD
Director, Center for Space Exploration Technology Research
[Formerly Combustion and Propulsion Research Laboratory]
Associate Professor, Mechanical Engineering
The University of Texas at El Paso
500 West University, Engineering M- 305, El Paso, Texas 79968
Tel: 915 747 6905, Fax: 915 747 5019, E-mail:ahsan@utep.edu

Research Assistants:
Bidhan Dam
Gilberto Corona
Vishwanath Ardha

Preface

This is the final technical report on DOE Grant DE-FG26-08NT0001719 entitled "Effects of Combustion-Induced Vortex Breakdown of Flashback Limits of Syngas-Fueled Gas Turbine Combustors". Technical work supported by this grant described in parts in the masters thesis of Bidhan Dam and Vishwanath Ardha. The results presented in the report are also included in two journal articles titled: "*Flashback Propensity of Syngas Fuels*, " Fuel, Vol. 90(2011), No. 2, pp. 618-625 and "*An Experimental Investigation of Combustion Induced Vortex Breakdown Flashback in a Swirl Stabilized Burner*," Fuel, accepted for publication in 2011. The journal papers are coauthored by Ahsan Choudhuri, Norman Love, Bidhan Dam, and Gilberto Corona.

I. Overview

Turbine combustors of advanced power systems have goals to achieve very low pollutants emissions (NO_x < 2-ppm), fuel variability, and fuel flexibility [1]. Future generation gas turbine combustors should tolerate fuel compositions ranging from natural gas to a broad range of syngas without sacrificing operational advantages and low emission characteristics [1,2]. However, issues of fuel variability and NO_x control through premixing also bring a number of concerns, especially combustor flashback and flame blowout. Flashback is a combustion condition at which the flame propagates upstream against the gas stream into the burner tube. Flashback is a critical issue for premixed combustor designs, because it not only causes serious hardware damages but also increases pollutant emissions. The presence of hydrogen in syngas significantly increases the potential for flashback. Due to high laminar burning velocity and low lean flammability limit, hydrogen tends to shift the combustor operating conditions towards flashback regime. Even a small amount of hydrogen in fuel mixtures triggers the onset of flashback by altering the kinetics and thermophysical characteristics of the mixture.

In a series of papers, Settlemayer and co-workers [3-5] discussed a number of flashback modes taking place in a swirl stabilized lean premixed turbine combustor. They identified flashback to be initiated by one of the following four causes:

(i) flame propagation in the boundary layer,
(ii) turbulent flame propagation in the core flow,
(iii) violent combustion instabilities, and
(iv) combustion induced vortex breakdown (CIVB).

I. a Boundary Layer Flashback

In the case of boundary layer flashback, the flame propagates upstream when its normal burning velocity exceeds the local flow velocity. This type of flashback generally occurs close to the wall where a no slip boundary condition exists. In their classical study, Lewis and von Elbe [6] studied flame-wall interactions and used flame quenching theories to explain the occurrence of flashback in boundary layers. For a flame stabilized over a circular tube burner, they explained the flashback phenomena by 'critical boundary velocity gradient' and calculated the value of that for natural gas-air mixture at room temperature and pressure using various cylindrical tube diameters. If the velocity profile in the boundary layer of the flame is linear, the velocity gradient, g, can be defined as:

$$\mathbf{g} = \frac{\mathbf{u_b}}{\mathbf{y}} \qquad \textbf{(1)}$$

where y is the distance from the stream boundary and u_b is the unburned gas velocity. Equation (1) is generally true for a large diameter burner tube. The velocity gradient (g) decreases with the decrease in unburned gas velocity and the flame stabilizes at a position close to the burner lip. When the unburned gas velocity becomes smaller than the burning velocity (S_L) the flame

propagates downstream against the unburned gas flow. This condition is referred to as the boundary layer flashback and the critical value of g at which the flashback condition is observed is denoted by g_F. From experimentally determined flow rates, Lewis and von Elbe [6] calculated g_F for natural gas-air mixture at room temperature and pressure for various cylindrical tube diameters. The critical value, g_F, primarily depends on the laminar burning velocity (S_L) and can be expressed as:

$$\mathbf{g_F = \frac{S_L}{d_p}} \quad \textbf{(2)}$$

Where d_p is the flame penetration distance which generally correlates with the quenching distance (d_q) as follows:

$$\mathbf{d_p = a d_q} \quad \textbf{(3)}$$

Where a is a burner constant. The quenching distance d_q again broadly depends on the laminar burning velocity and the mixture thermal diffusivity:

$$\mathbf{d_q = 2\sqrt{b}\,\frac{\alpha}{S_L}} \quad \textbf{(4)}$$

Where b is a burner scaling constant. Combining equations 2-4 yields

$$\mathbf{g_F = c\frac{S_L^2}{\alpha}} \quad \textbf{(5)}$$

Where

$$\mathbf{c = \frac{1}{2a\sqrt{b}}} \quad \textbf{(6)}$$

Recently, a detailed investigation of the boundary layer flashback for hydrocarbon fuels blends (CH_4-C_3H_8 and CH_4-C_2H_6) and hydrogen fuel blends (CO-H_2 and CH_4-H_2) was done by Davu el al. [7] and Choudhuri [8]. They showed that although the flashback propensity for hydrocarbon blends generally correlates with the flame velocity and stoichiometry of the fuel mixtures, flashback characteristics of syngas fuels were dominated by the kinetics of the hydrogen. The authors also showed that hydrocarbon fuel blends were found to be more susceptible to external excitation by acoustic forces for which flashback occurred even at much leaner conditions. In contrast, the flashback propensity of CO-H_2 flames with more than 5% H_2 were not significantly affected by external excitation.

If S_L and α are known it is possible to estimate the boundary layer flashback propensity of a fuel mixture, provided the value of c is available. However, boundary layer flashback data for fuel blends are scarce and the value of c is not readily available for various fuel mixtures.

I. b Turbulent Flame Propagation in the Core Flow

Turbulent flame propagation in the core flow occurs generally in highly swirling flow where local burning velocity supersedes local flow velocity. A highly swirling flow with Swirl Number, S > 0.7 extends the flame surface and triggers the onset of flashback along the burner axis [9].

Although specific literature on the effects of syngas compositions on flashback due to turbulent flame propagation is limited, the topic of turbulence-kinetics interactions is well studied and can be found in the following references [10- 12]. Other authors such as Candel [13] have also addressed various issues of turbulent flame propagation flashback in premixed combustion conditions.

I. c Violent Combustion Instabilities

Instability in the combustion chamber is commonly referred to as large-amplitude pressure fluctuations of acoustic nature [14] that takes place near-stoichiometric operation in high-power and lean-flammability low-emission combustors [15]. In general, complex non-linear interactions of pressure fluctuations along with periodic heat release and flow hydrodynamics collectively induces such instabilities in the combustion chamber. Flame flashback due to instabilities can occur in various combustor conditions even when flame propagation in the boundary layer is not possible [16]. A number of investigators including have examined the effects of combustion oscillation on laminar and turbulent flame propagation and have shown that these instabilities can cause the flame to propagate upstream periodically during the pulsation cycles [17 - 19].

I. d Combustion Induced Vortex Breakdown (CIVB)

Sattelmayer and coworkers [3-5] have demonstrated CIVB to be the prevailing flashback mechanisms in swirl stabilized gas turbine combustors. Usually, the dynamics of swirl flows are complex due to time varying 3D nature of their precessing vortex core. The stability of swirl flows and their subsequent breakdown into reverse flow are primary controlled by swirl and Reynolds Number [20]. An increase in azimuthal velocity in relation to axial velocity results in vortex break down and the formation of a low or negative flow region ahead of it [21]. The flame then propagates upstream causing the vortex breakdown region to move further upstream. As this process continues, the flame propagates further and further upstream, forcing flashback to occur even if the burning velocity everywhere is less than the flow velocity.

Boundary layer and turbulent flame propagation flashback are topic of classical interest generally described with sufficient precision through analytical theories and experimental determinations of laminar and turbulent burning velocities for single component fuels. However, flashback processes get increasingly complicated in the case of swirling flows, thus the two aforementioned mechanisms cannot adequately describe the flashback propensity of most practical combustor designs. In those cases, flashback may also take place through combustion instabilities and CIVB. Additionally, the presence of hydrogen in syngas significantly increases the potential for flashback. Due to high laminar burning velocity and low lean flammability limit, hydrogen tends to shift the combustor operating conditions towards flashback regime. Even a small amount of hydrogen in a fuel blend triggers the onset of flashback by altering the kinetics and thermophysical characteristics of the mixture. The presence of hydrogen in the fuel mixture also modifies the response of the flame to the global effects of stretch and preferential diffusion [22]. Noble and co-workers [23] recently reported an extensive investigation of the fuel composition effects on the combustion instability driven flashback process in swirl stabilized combustors.

I. e Project Interests

Despite its immense importance in fuel flexible combustor design, little is known about the magnitude of hydrogen addition and syngas usage on boundary layer and CIVB flashback mechanisms. Additionally, most of the investigations carried out previously were focused on methane combustion. This report presents a detailed investigation on boundary layer and CIVB flashback limits of various H_2-CO fuel blends and actual syngas mixtures. The key objective involves providing a better understanding of the effect of different fuel constituents, burner configuration, and swirl strength on flashback propensity induced by boundary layer and CIVB flashback.

II. Experimental Methodology

II. a Boundary Layer Flashback Tubular Burner System

The flashback burner system shown in Figure 1 has four primary components: (i) mixing manifold, (ii) flow excitation hub (base, speaker and speaker housing), (iii) flow conditioner (honeycomb, honeycomb housing and wire mesh), and (iv) burner tube assembly (converging nozzle, glass tubes, glass tube adapters, adjustable supports, and c-clamps). The converging nozzle section seamlessly merges with the adapters to accommodate glass tubes of different diameters (10.6 mm, 7 mm and 6 mm). The fuel and air enter into the manifold through four alternate injection holes. The fuel-air mixture then passes through the flow conditioning section to eliminate injection induced flow irregularities and to insure laminar flow through the burner tube. Since the burner system is also designed to analyze the flashback with external excitation, the bottom part of the injection manifold opens to an optional flow excitation hub section.

Figure 1: Experimental setup for boundary layer flashback

The flame was ignited at a flow rate higher than the expected critical flow rate. During an experiment, the flow rate was reduced in small increments while keeping the composition constant until the flame propagated back into the tube. A high-speed direct video imaging system was used to confirm the flashback condition. The critical boundary velocity gradient g_F for different compositions of hydrocarbon fuel blends and syngas were calculated using the following relation

$$\mathbf{g_F = \frac{4\mathbb{V}}{\pi d^3}} \qquad \textbf{(7)}$$

Where V is experimentally measured volumetric flow rate at flashback condition and d is the tube diameter. The volumetric flow rate for a particular tube diameter and mixture composition at which the flame propagates down the burner tube were defined as the critical flow rate V. In order to draw the flashback propensity map, critical volumetric flow rate for flashback at different mixture compositions in cylindrical tubes of various diameters were measured.

II. b Combustion Induced Vortex Breakdown Swirl Flow Combustor Rig

A modular laboratory scale gas turbine combustor was constructed and used for the present investigation. The combustor rig has three configurable modules: (i) inlet manifold with static mixer, (ii) swirl burner with mixing tube, and (iii) optically accessible combustion chamber, see Figure 2. The module integrates a pilot flame ring with a mixture of methane and air. The swirl burner module is fitted with a quartz mixing tube. The quartz glass tube is needed for the high speed imaging of flashback inside the premixer. Fuel and air enter the inlet manifold through five alternate injection holes. The fuel-air mixture then passes through the static mixture section to eliminate injection induced flow irregularities and to ensure proper mixing of air and fuel. The burner module can accommodate both centerbody and hubless swirlers. In the present study, experiments were carried out using centerbody swirlers. During conducting experiments, a circular sleeve was fitted inside the inlet of the combustion chamber; this allows the air-fuel mixture to enter the combustion chamber through the passage between the sleeve and the centerbody of the swirler. As a result, the mixture flow does not experience any pressure drop due to the divergence at the inlet of the combustion chamber.

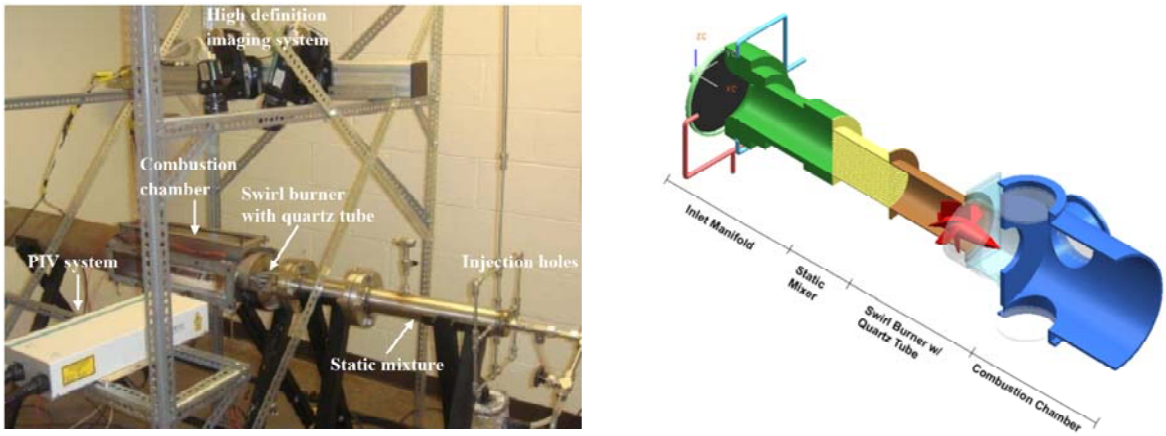

Figure 2: (a) Modular swirl burner facility and (b) the complete experimental setup

Air was supplied to the rig through a high pressure (maximum 900 cfm of air at 125 psi) rotary screw type compressor. Research grade fuels were delivered to the combustor from pressurized tanks. Precision metering valves in conjunction with low-torque-quarter-turn plug valves were used to control and meter fuel and air flow rates. A bank of digital mass flow controllers were used to measure mass flow rates of fuels and air.

The combustion chamber is constructed in a rectangular-type cross-section whose side-walls are made up of quarts glass to provide optical access inside it. The chamber is also fitted with solenoid controlled exhaust port and emergency pressure relief systems for safety purposes. The

entire combustor rig is positioned horizontally and can be operated at a maximum pressure of 624 kPa with a prescribed design safety factor.

A high resolution direct imaging system (Phantom v310 camera, with a resolution of 1280 x 800 at 3250 fps and a maximum frame rate of 500,000 fps) and a high speed PIV system (20 kHz) were simultaneously used with intensified camera systems (Hamamatsu C10880, with maximum repetition frequency of 200 kHz) to capture the flashback sequences and to analyze the reacting and non-reacting particle velocity flow-fields. All the equipments were synchronized with Dantec Dynamics software. In PIV experiments, aluminum particles were used as seeding elements. Experimental uncertainties (bias + random errors) of the present measurements were less than ±1.0% of the mean value. Additionally, all H_2-CO mixture compositions reported here are in volumetric percent.

III. Numerical Model

III. a Governing Equations

The governing equations for LES are obtained by applying a filtering operator Eq. (8) to the Navier-Stokes equations. The effect that this filtering operator has is that the scales smaller than the filter width are averaged out and their effect is modeled. The filtering operator and the resulting incompressible governing equations for LES are presented in Eqs (8-12) [24].

$$\overline{\emptyset}(\mathbf{x}) = \int_D \emptyset(\mathbf{x}')\mathbf{G}(\mathbf{x},\mathbf{x}')\mathbf{dx}' \tag{8}$$

$$\frac{\partial \rho}{\partial t} + \frac{\partial}{\partial x_i}(\rho \bar{u}_i) = 0 \tag{9}$$

$$\frac{\partial}{\partial t}(\rho \bar{u}_i) + \frac{\partial}{\partial x_j}\left(\rho \bar{u}_i \bar{u}_j\right) = \frac{\partial}{\partial x_j}\left(\sigma_{ij}\right) - \frac{\partial \bar{p}}{\partial x_i} - \frac{\partial \tau_{ij}}{\partial x_j} \tag{10}$$

Where

$$\sigma_{ij} \equiv \left[\mu\left(\frac{\partial \bar{u}_i}{\partial x_j} + \frac{\partial \bar{u}_j}{\partial x_i}\right)\right] - \frac{2}{3}\mu \frac{\partial \bar{u}_k}{\partial x_k}\delta_{ij} \tag{11}$$

And

$$\tau_{ij} \equiv \rho\overline{u_i u_j} - \rho \bar{u}_i \bar{u}_j \tag{12}$$

There are many subgrid-scale and filtering operators currently available. Based on initial simulation runs, selection of different models did not significantly affect results. For the combustion model, however, it was found to significantly affect the model output. For this portion of the report the Smagorinsky-Lilly subgrid-scale model was used to compute the subgrid-scale stresses from Eqns (13-16) [24].

$$\tau_{ij} - \frac{1}{3}\tau_{kk}\delta_{ij} = -2\mu_t \bar{S}_{ij} \tag{13}$$

Where

$$\bar{S}_{ij} \equiv \frac{1}{2}\left(\frac{\partial \bar{u}_i}{\partial x_j} + \frac{\partial \bar{u}_j}{\partial x_i}\right) \tag{14}$$

In the Smagorinsky-Lilly model, the turbulent viscosity is modeled from

$$\mu_t = \rho L_s^2 |\bar{S}| \tag{15}$$

Where

$$|\bar{S}| \equiv \sqrt{2\bar{S}_{ij}\bar{S}_{ij}} \tag{16}$$

L_s is computed using

$$L_s = \min(\kappa d, C_s \Delta) \tag{17}$$

For the preliminary numerical study two models were selected. The first model uses species transport with eddy dissipation concept for treating the turbulence-chemistry interaction with detailed chemical mechanisms. Complete reaction mechanisms required extensive computational power and single step mechanisms could not accurately predict combustor temperatures and emission characteristics. Thus a reduced mechanism with a limited number of species and reaction steps was used with the model [25]. The software used is FLUENT which was coupled with CHEMKIN. FLUENT uses a convection-diffusion approach, Eq. (18), to solve for the conservation of chemical species were the net rate of production of chemical species *i* (R_i) is modeled by Eq. (19) [24]

$$\frac{\partial}{\partial t}(\rho Y_i) + \nabla \cdot (\rho \vec{u} Y_i) = -\nabla \cdot \vec{J}_i + R_i + S_i \tag{18}$$

$$R_i = \frac{\rho(\xi^*)^2}{\tau^*\left[1-(\xi^*)^3\right]}\left(Y_i^* - Y_i\right) \tag{19}$$

Where

$$\xi^* = C_\xi \left(\frac{\nu\varepsilon}{k^2}\right)^{1/4} \tag{20}$$

And

$$\tau^* = C_\tau \left(\frac{\nu}{\varepsilon}\right)^{1/2} \tag{21}$$

The mass diffusion is modeled by

$$\vec{J}_i = -\left(\rho D_{i,m} + \frac{\mu_t}{Sc_t}\right)\nabla Y_i - D_{T,i}\frac{\nabla T}{T} \tag{22}$$

Another model used for the study utilizes OpenFOAM and the turbulent premixed combustion solver XiFoam which is based on the reaction regress variable approach. Here the domain consists of regions of unburned reactants and regions of combusted products. The extent of combustion is measured by means of a regress variable that takes values between 0 and 1, where a value of 0 represents the presence of completely burnt products and a value of 1 indicates

unburned gases; the transition between these values marks the flame front. The model assumes that the flame propagates as a laminar flame being wrinkled due to the interaction with turbulence[4]. To model the flame front, OpenFOAM solves a transport equation for the density-weighted mean reaction regress variable b presented in Eq. (23).

$$\frac{\partial}{\partial t}(\rho b) + \nabla \cdot (\rho \vec{u} b) - \nabla \cdot (\rho D \nabla b) = -\rho_u S_u \Xi |\nabla b| \tag{23}$$

Where

$$b = 1 - c \tag{24}$$

And c is a progress variable that can be set with any quantity that is bounded by a single value in the burned and unburned gas, in this case temperature.

$$c = \frac{T - T_f}{T_b - T_f} \tag{25}$$

III. b Grid Development

The grid domain used for the present study has a diameter of 50 mm for the burner tube and 150 mm for the combustion chamber. The computational domain used an axial length of 75 mm and 230 mm for the burner tube and the combustion chamber, respectively. These dimensions were selected based on the experimental combustor which has the same dimensions. The model used a 12 vane swirler with a Swirl Number of 0.97 placed near the air inlet boundary, Figure 3. After the mesh was generated, the appropriate boundary conditions were selected. The final 3 dimensional mesh contained 1,200,000 elements.

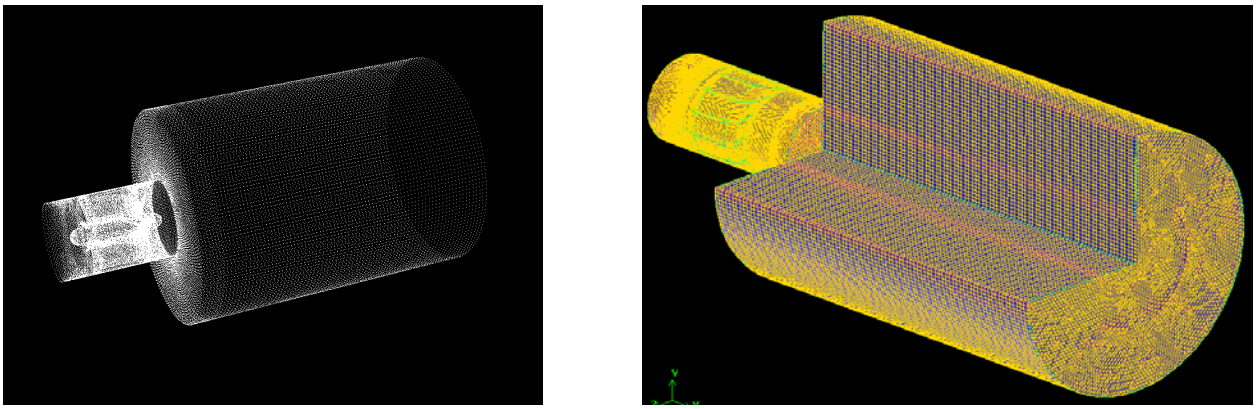

Figure 3: Computational domain (left) showing swirler at combustor inlet and (right) showing grid cells cross-section

IV. Results and Discussions

IV. a Boundary Layer Flashback

Visual Observation and Qualification of the Test Apparatus

Flame images at a typical flashback condition are presented in **FIGURE 4**. The flame attached to parts of the burner inner surface due to a slow locally unburned velocity near the wall. The partial flame inside the burner tube heated the tube wall and increased the temperature of the upstream fuel-air mixture. The flame then gradually moved inside the burner causing a flashback. The critical velocity gradients (g_F) for a natural gas composition of 81.8% CH_4, 17.7% C_2H_6 and 0.5% N_2 were measured to reproduce the data provided by the Lewis and von Elbe [6] work. **FIGURE 5** presents the measured g_F values in the present study plotted with the Lewis and von Elbe's measurements. Present measurements agree fairly well with the previously reported data.

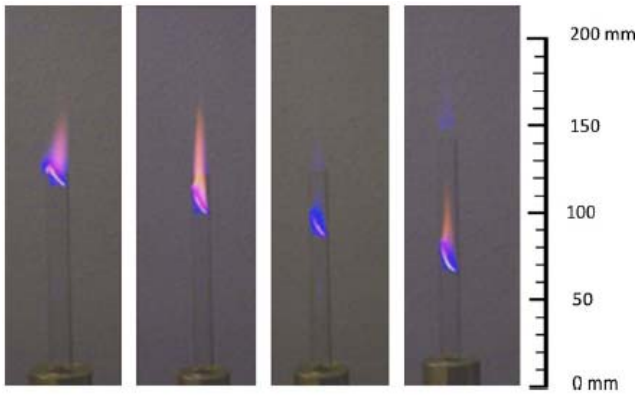

Figure 4: Boundary Layer Flashback Process

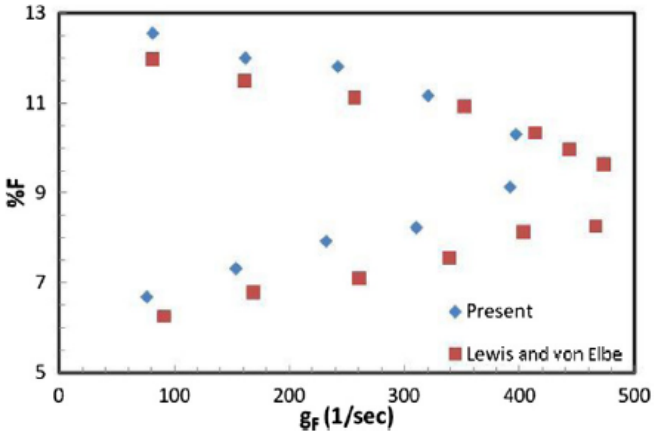

Figure 5: Comparisons of present measurements and data from Ref [6]

Effects of Fuel Composition

FIGURE 6 shows critical velocity gradients of H_2-CO mixtures at different H_2 concentrations and mixture equivalence ratios (%F). The boundary layer flashback propensity, indicated by higher values of g_F, increased nonlinearly for higher hydrogen concentrations in the fuel mixture. The largest differences in g_F were observed near a 50% volumetric fuel composition, for fuel mixtures of 5%H_2-95%CO and 25%H_2-75%CO g_F values were 1435 and 2573 sec^{-1}, respectively. The effect of hydrogen addition on flashback was especially significant at rich conditions. This was due to the presence of hydrogen in fuel mixtures which creates the necessary branched chain reactions to accelerate the flame propagations. The H_2 in the mixtures supplies the necessary active radicals and atoms such as OH, O and H and their diffusion rates into the unburned gas determines the magnitude of flame propagation velocity. However, it is interesting to note that the increase in g_F with H_2 concentration in lean mixtures is small compared to fuel rich mixtures. Thus the sharp increase in flashback propensity of high hydrogen content mixtures may be due to the effect of preferential diffusion. Recent investigations have suggested that the change in fuel compositions can cause the flame front wrinkling even without the presence of turbulence [23,26,27]. High molecular diffusivity of hydrogen can change the local equivalence ratio in high hydrogen content mixtures and thus can increase the local flame speed. This may be the reason of a sudden increase in flashback propensity at rich conditions.

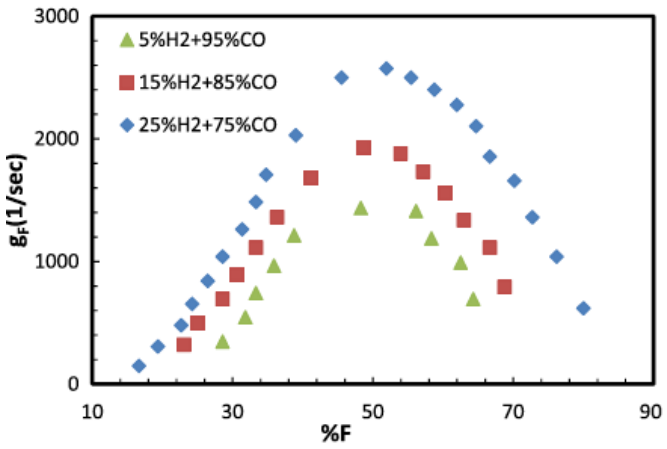

Figure 6: Critical velocity gradients at different mixture compositions of H_2-CO

Figure 7 presents the critical velocity gradients of H_2-CH_4 mixtures for different H_2 concentrations and mixture equivalence ratios (%F). Note that the flashback data is presented for 3 to 15% fuel composition and up to a g_F value of 800. This range was significantly less than that of H_2-CO, resulting from the more narrow flammability limits of the fuel mixture. The boundary layer flashback behavior of the H_2-CH_4 mixtures reached a maximum at approximately 8% fuel concentration, decreasing thereafter. The effect of hydrogen addition on laminar burning velocity is observed to be significant, particularly at lean conditions. At higher fuel concentrations (above 9%), however, the effect of the addition of hydrogen on laminar burning velocity was offset by the much higher overall thermal diffusivity. Thus the addition of more H_2 to the mixture did not significantly affect g_F values above 9% fuel concentration.

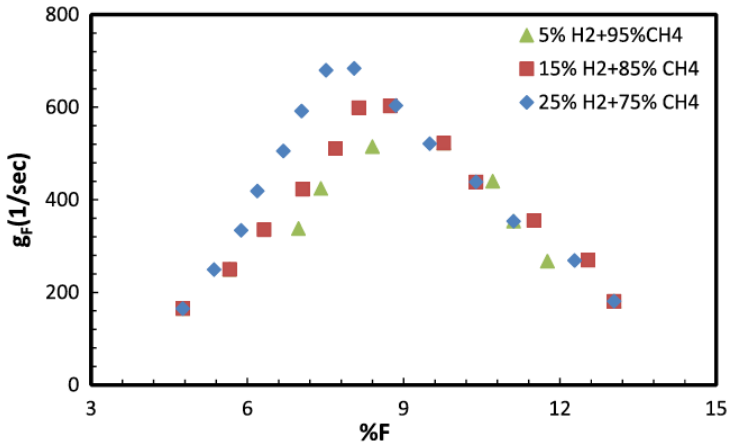

Figure 7: Critical velocity gradients at different mixture compositions (H_2-CH_4)

Figure 8 shows the effects of N_2 dilution (a minor constituent of syngas fuels) on the boundary layer flashback propensity of H_2-CO mixtures. Experiments were performed with a simultaneous increase in both H_2 and N_2 concentrations. The objective was to understand the comparative effects of H_2 and N_2 concentrations on flashback propensity of syngas fuel flames. Figure 6 indicates that the increase in H_2 concentration has a dominant effect on the flashback propensity and thus the g_F value. This same trend was also observed for an increase of H_2 and N_2 concentrations in the fuel mixture, Figure 8. However, unlike undiluted fuel mixtures of H_2-CO, where the differences in g_F values were greater at fuel-rich conditions, diluted mixtures saw an increase in g_F for both fuel-lean and fuel-rich conditions. This indicates that the boundary layer flashback propensity of H_2-CO mixtures is dictated by a complex interaction of laminar flame velocity, thermal transport and preferential diffusion.

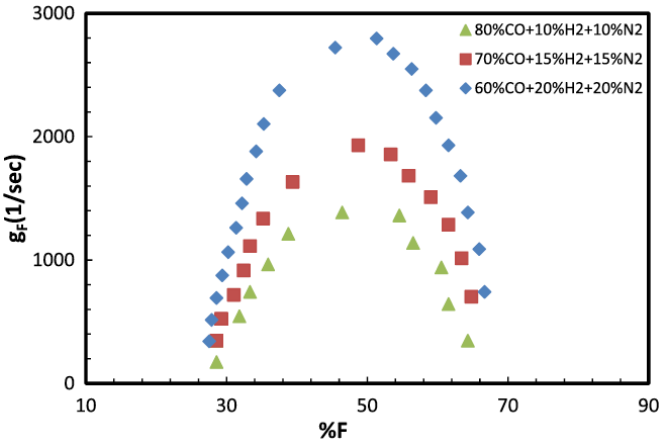

Figure 8: Critical velocity gradients of diluted H_2-CO mixtures

Effects of Burner Diameter

The burner tube diameter has a scale effect on the experimental determination of critical velocity gradients, as shown in Eq (4). Figure 9 shows critical velocity gradients of 25%-75% H_2-CO measured at three different tube diameters: 6, 7, and 10.6 mm. It is interesting to note that the effect of burner diameter is smaller for lean mixtures. However, for a fuel rich mixture a larger burner diameter results in a lower g_F value. Although it is expected that the smaller diameter lowers the g_F value because of quenching effects, the experimental values show the opposite. For a rich condition the 10.6 mm burner diameter has lower g_F values in compared to 6.0 and 7.0mm burner tubes. It seems that the cooling of a partially entered flame front due to extended surface area of large burner tube determined the burner scale effects.

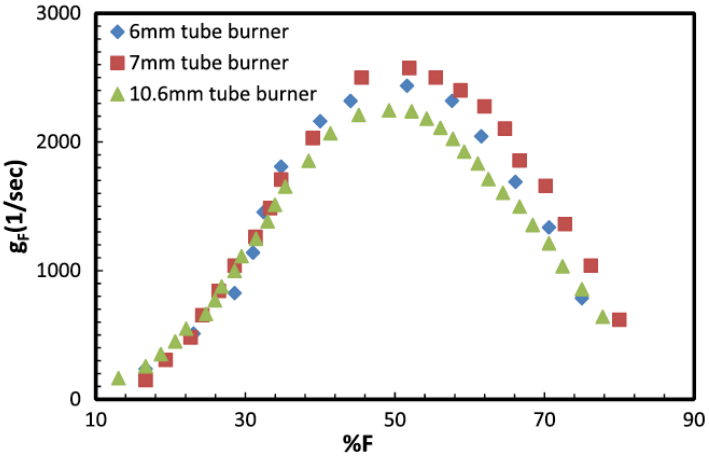

Figure 9: Critical velocity gradients of 25-75% H_2-CO mixtures measured at different burner diameters

FIGURE 10 shows the critical velocity gradients of 25%-75% H_2-CH_4 measured at three different tube diameters: 6, 7, and 10.6 mm. As discussed in the previous section, the H_2-CH_4 critical velocity gradients are less affected by the increase of H_2 percentage for rich conditions. At lean conditions, however, it is observed that the 6mm and 10.6mm burner tubes have significantly higher g_F values than the 7mm burner tube. For the 6mm and 10.6mm burner tubes it is expected that the heat release factor dominates over the quenching effect. The 7mm diameter tube showed lower g_F values than either tube. This could be occurring at a critical burner diameter since flashback propensity effects were minimized. More investigation is needed to determine the reason for significantly lower g_F values using this burner.

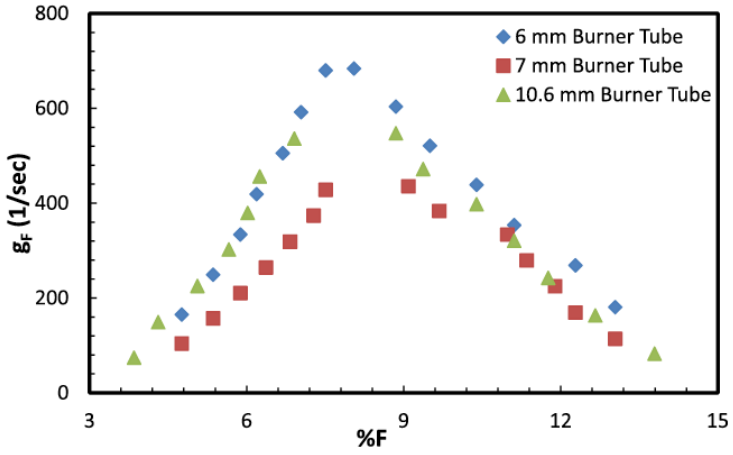

Figure 10: Critical velocity gradients of 25-75% H_2-CH_4 mixtures measured at different burner diameters

FIGURE 11 shows the burner scaling effects on N_2 diluted H_2-CO mixtures. It appears that the N_2 diluted mixtures exhibit a strong burner scaling effects due to an accelerated quenching of active radicals by inert third-body collisions (N_2 molecules and extended tube surface area).

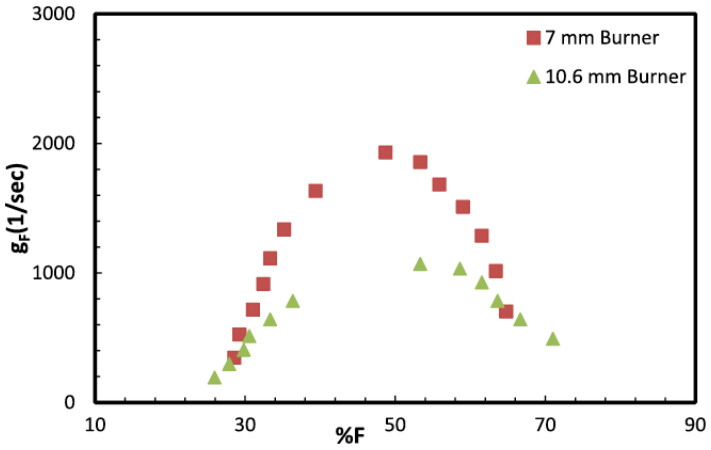

Figure 11: Critical velocity gradients of 15-60-15% H_2-CO-N_2 mixtures measured at different burner diameters

Scaling with the Laminar Burning Velocity

Equation (5) shows a generally accepted scaling relation between g_F, S_L and α. It is important to note that the scaling constant, c, in Equation (5) is related to the burner dimension and does not necessarily capture the effects of fuel compositions. During the initial formulation of Equation (5) it was assumed that the fuel effects were captured in the variation of S_L and α values. However, the measured values of g_F at different concentration of H_2 in H_2-CO mixtures clearly indicate that other transport processes such preferential diffusion may also have significant

effects on boundary layer flashback propensity. Thus, a higher order formulation may be necessary to capture both fuel and burner effects.

Figure 12 shows the measured g_F values from a 6 mm diameter burner plotted against computed S_L and α values from the CHEMKIN kinetic code, using the GRI 3.0 mechanism. The data were then fitted using the scaling relation. The g_F values of 5%-95%, 15%-85%, and 25%-75% H_2-CO mixtures somewhat agree with the scaling relation and yielding an average c value of 0.4, as seen in Table 1.

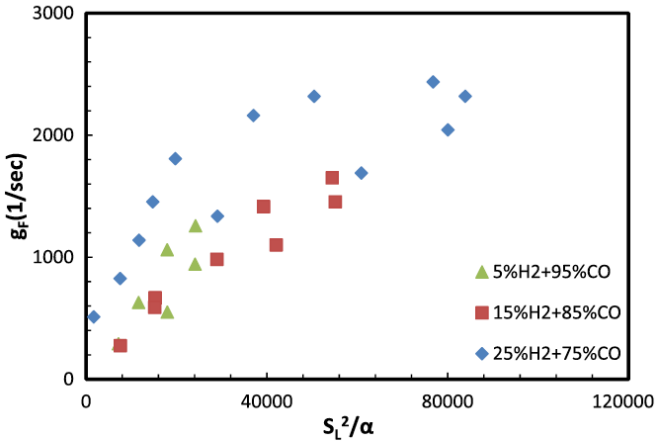

Figure 12: Scaling of g_F and S_L^2/α (6.0 mm burner)

Table 1: Scaling of g_F and S_L^2/α for H_2-CO mixtures (6.0mm burner)

Composition	Scaling Factor (c)	R^2 Value
5% H_2 + 95% CO	.04	.7
15% H_2 + 85%CO	.025	.9
25%H_2 + 75%CO	.049	.8

Figure 13 shows the g_F values of 25%-75% H_2-CO mixture measured at different burner diameters and plotted against the scaling ratio S_L^2/α. It appears that at a lower S_L^2/α ratio there are insignificant effects of burner diameters, however the data diverge at a higher S_L^2/α ratio. Figure 14 shows the g_F values measured at a 6 mm diameter burner with different H_2-CH_4 mixtures. Using these data a plot of g_F at 25%H_2-75%CH_4 for different burner diameters was fitted using the scaling relation, Figure 15. The g_F values of 6, 7, 10.6mm diameter burners agreed with the scaling relation and yielding an average c value of 0.044, Table 2.

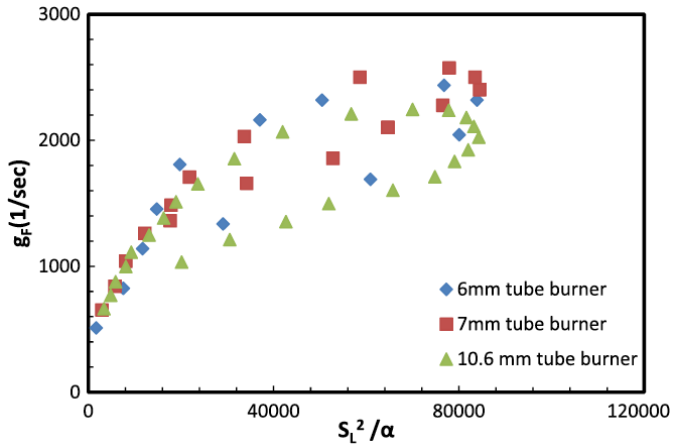

Figure 13: Scaling of g_F and S_L^2/α (25-75% H_2-CO mixture).

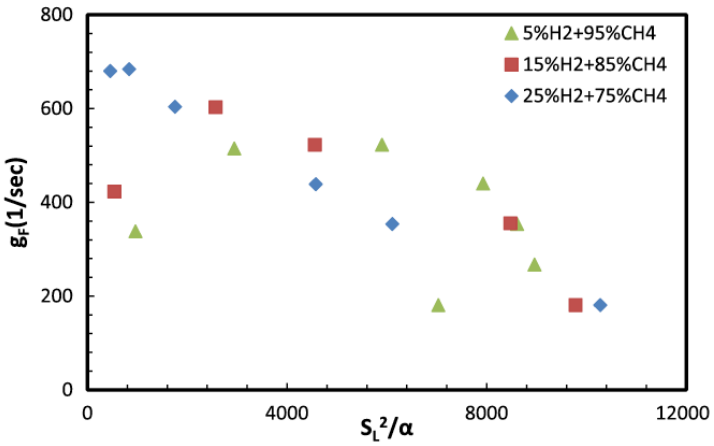

Figure 14: Scaling of g_F and S_L^2/α (6.0 mm burner)

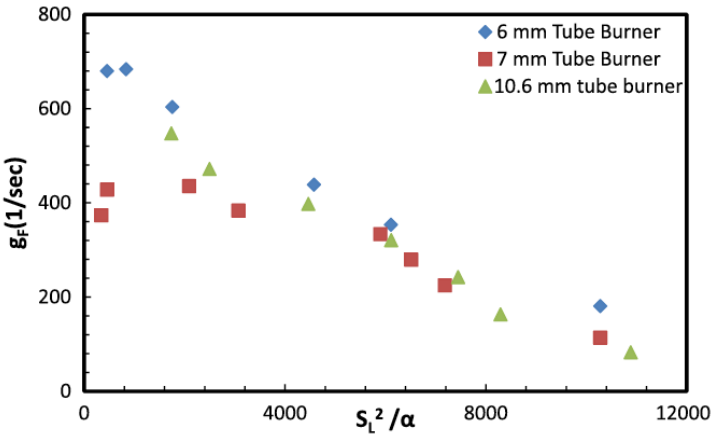

Figure 15: Scaling of g_F and S_L^2/α (25-75% H_2-CH_4 mixture).

Table 2: Scaling of g_F and S_L^2/α for 25%H_2-75%CH_4 mixtures with different burner

Burner diameter (mm)	Scaling Factor (c)	R^2 Values
6	.053	.98
7	.029	.86
10.6	.05	.98

IV. b Combustion Induced Vortex Breakdown in a Swirl Stabilized Burner

Experimental measurements of the swirl-stabilized flame were performed for a wide range of mixture compositions, equivalence ratios, and airflow velocities. Initially, an experiment was carried out with a methane (CH_4)-air mixture and the results used as a baseline for other synthetic gas fuel mixtures. The magnitude of the fuel effects on CIVB flashback for various H_2-CO mixtures and actual syngas compositions were then documented. Two centerbody swirlers, one with 6 vanes (S = 0.71) and the other with 12 vanes (S = 0.97), were employed. Using the flashback data for the two swirlers, a comparison of the flashback propensity of each was obtained.

To attain flashback, the flow rates of both fuel and air were initially adjusted so that the flame was stabilized completely inside the combustion chamber. The airflow rate was then slowly decreased while maintaining the same fuel flow rate. Thus, the premixed fuel-air mixture became more fuel rich for lower airflow rates. At a critical condition the flame propagated upstream and stabilized inside the burner tube. The flow rates of fuel and air at the critical condition were recorded for used for data mapping. Each experiment was repeated six times and used to determine the experimental uncertainties based on a Student's t-distribution at a 95% confidence interval.

To investigate the corresponding reacting flow fields, the PIV system was simultaneously used. The analysis of the flow field in both stable and flashback conditions helped identifying the mechanism that caused a stable flame to undergo flashback. The images obtained from PIV measurements provided the instantaneous velocity information with high spatial resolution over a period of time. However, in some cases of the present investigation, it was hard to identify various flow phenomena occurring within reacting flow fields from the raw PIV images. The use of Proper Orthogonal Decomposition (POD) analysis in those cases resulted in better flow-visualization images. For example, the first two images in Figure 16 represent the reaction flow field for a CH_4-air mixture flame at a stable condition, particular equivalence ratio, and S = 0.97.

The first image (a) shows the vector flow field without POD analysis and the second image (b) represents the same but with POD analysis. A comparison of these two images reveals that frame (b) shows the formation of recirculation zones enclosed by two high-velocity flame regions (residing close to the combustion chamber wall). The corresponding recirculation and high-velocity flame zones were also observed in the third image in Figure 16, which represents the

scalar flow field of the same condition. Therefore, the reaction flow fields of various fuel mixtures were based on scalar imaging based on POD processed raw images.

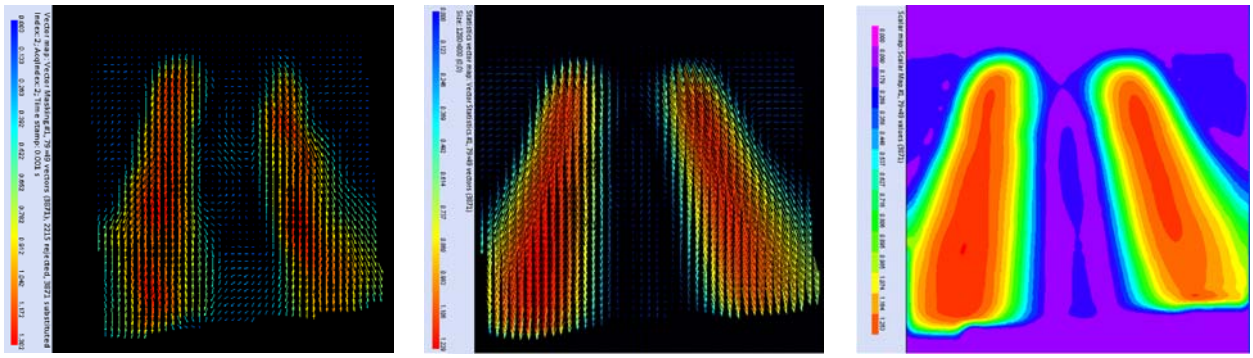

(a) (b) (c)

Figure 16: Reaction flow field for methane-air mixture flame in stable condition for Swirl Number, S = 0.97: (a) vector image without POD, (b) vector image with POD, and (c) scalar image with POD.

Visual Identification of CIVB Flashback

The images shown in Figure 17 represent a series of sample photographs (acquired by the digital imaging system) illustrating how a flame, starting from a stable state experiences flashback due to CIVB. Figure 17 shows that initially the flame is stabilized in front of the swirler, it then moves slowly upstream of the centerbody and starts oscillating with an increase in the equivalence ratio. The frequency of oscillation increases at higher equivalence ratios. The flame then stabilized upstream of the centerbody with an increase in the equivalence ratio. At the final point the flame was identified as flashback; demonstrated by the prominence of the centerbody compared to the previous frames.

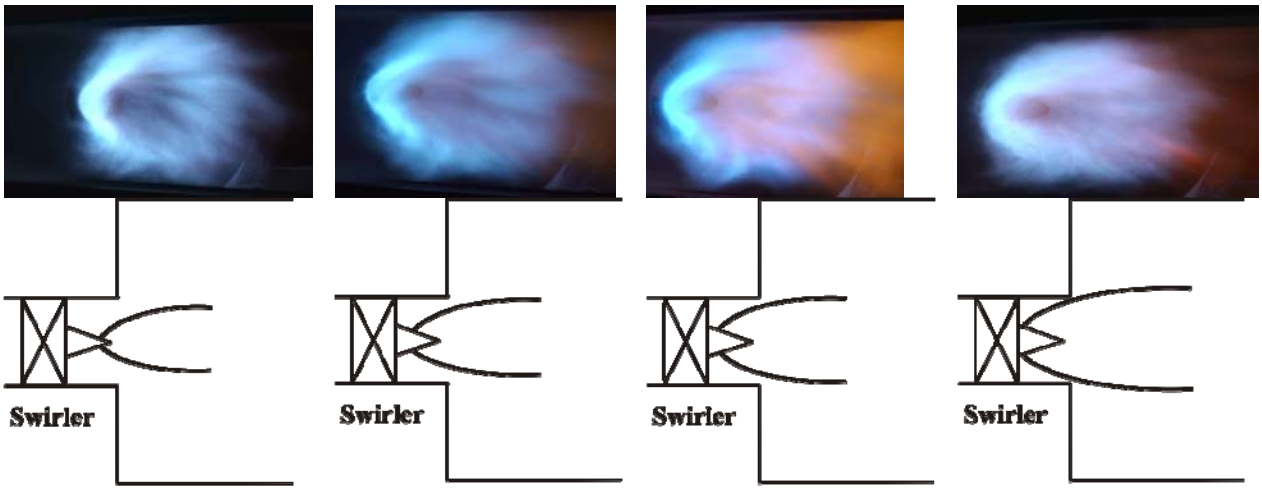

Figure 17: Sequence of a typical flashback phenomenon caused by CIVB with the upper row representing the photographic sequence and the lower row representing the same but by approximate lines only (not to scale).

Isothermal Flow-Field

A set of non-reacting experiments were performed using air seeded with magnesium oxide particles. Figure 18 shows a velocity vector image of the non-reacting flow field at an air mass flow rate of 6 g/s and S = 0.97 obtained by the PIV system.

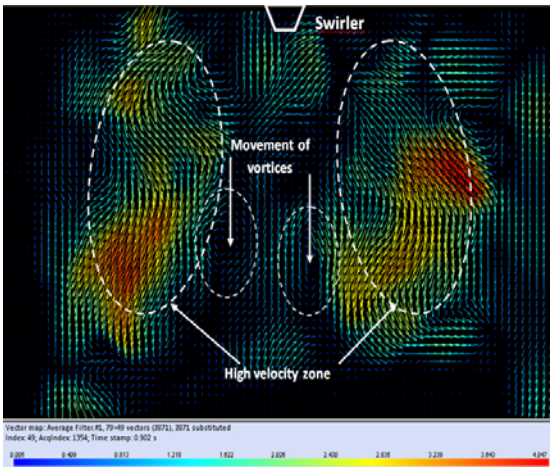

Figure 18: Non-reacting flow field for air flow with a flow rate of 6 g/s and Swirl Number S = 0.97

The swirler generated a gradually expanding flow area downstream of the burner. High velocity flow regions near the combustor walls provided enough space for recirculation of flow which contained vortices that propagated downstream through the recirculation zones. Thus, two high velocity flow regions near the combustion chamber walls with strong recirculation zones were observed. For reacting portion of the experiments this flow behavior is thought to assist in the stabilization of the flame near the swirler tip.

Reacting Flow/Methane-Air Combustion

The flashback limits for combustion of methane and air in the swirl stabilized combustor for a Swirl number of 0.97 is shown in Figure 19. From the figure it can be seen that the methane flame has the tendency to increase its flashback propensity with increasing airflow rate up to approximately 3 g/s for this combustor. As airflow rate was increased, the flashback propensity of the flame decreased.

Changes in the flame flow field during a typical flashback event is shown in Figure 20. At lower equivalence ratio the high-velocity flame stabilized close to the combustion chamber walls allowing the low-velocity recirculation zones to form between them. As equivalence ratio increased from a to b disturbances between the recirculation zone and flame tip were observed causing the volume between the recirculation zones to reduce. At a critical equivalence ratio the flame propagated upstream distorting the recirculation zones; c represents the flashback condition.

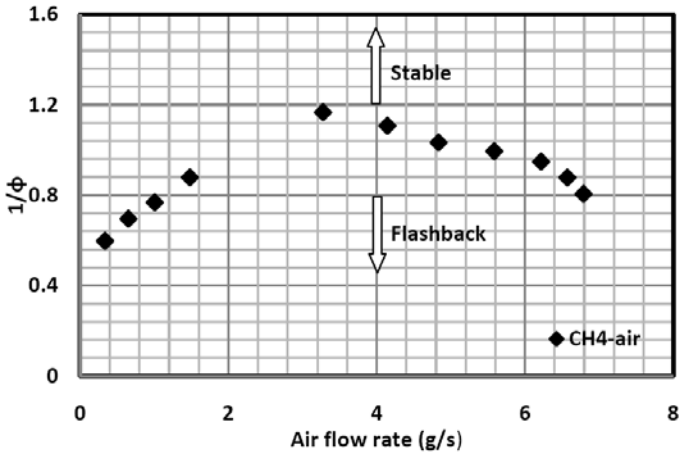

Figure 19: Flashback limits for methane-air flame in the swirl stabilized combustor with S = 0.97

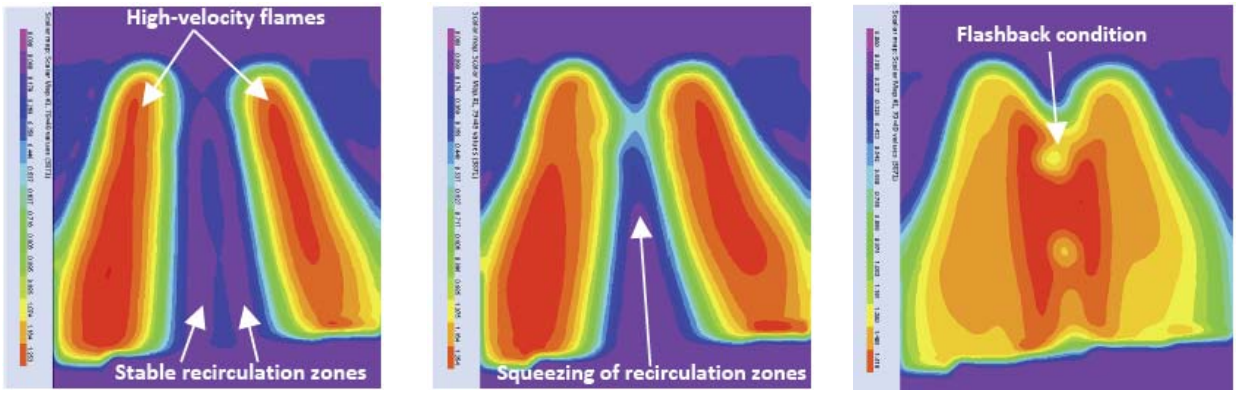

(a) (b) (c)

Figure 20: Change in the reacting flow field during a typical CIVB flashback phenomenon for CH_4-air mixture with S = 0.97

Reacting Flow/ H_2-CO Mixture Combustion

Effect of Fuel Composition

Figure 21 shows the flashback limits for different H_2-CO compositions and methane at S = 0.97. The presence of even small concentrations of H_2 resulted in higher burning velocities which caused H_2-CO fuel mixtures to undergo CIVB flashback at leaner conditions. The increase of H_2 percentage changed the kinetics and the thermophysical characteristics of the mixture and accelerated flame propagation. Thus for a given air mass flow rate, the equivalence ratio at which CIVB flashback occurred decreased for fuels with higher H_2 concentrations. The effect of hydrogen in the fuel mixture on flashback limits for the same H_2-CO fuel compositions at a lower swirl number of S = 0.71 are also presented in Figure 22.

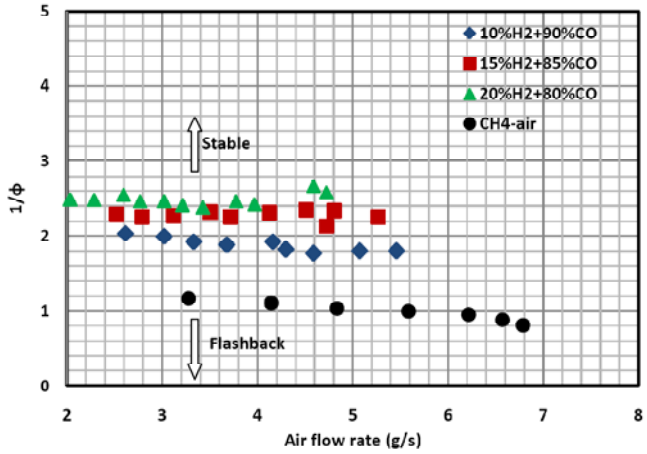

Figure 21: Comparison of the flashback limits of various H_2-CO mixture compositions with that of CH_4-air mixture for S = 0.97

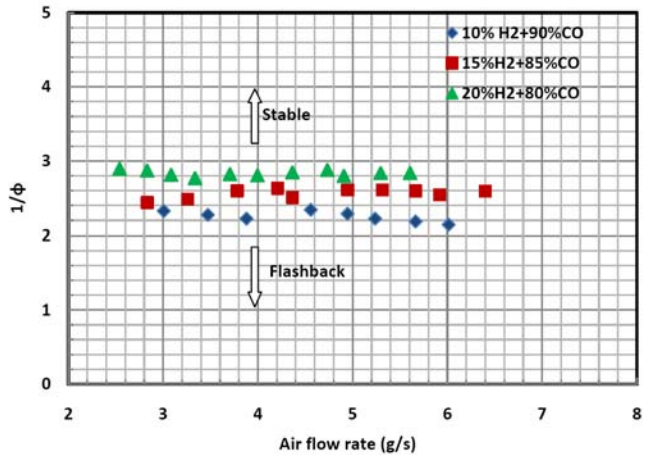

Figure 22: Flashback limits of various H_2-CO mixture compositions with S = 0.71.

Flow visualization images for 10%H_2 + 90%CO and 20%H_2 + 80%CO flow mixtures at S = 0.97 are shown in Figures 23 and 24. These figures demonstrate how the flow field changes from a stable flame to a CIVB driven flashback condition. For both cases flames were initially stabilized on the tip of the centerbody forming recirculation zones in the middle of the two high-velocity flame locations. Vortices V_1, V_2 and W_1, W_2 propagated through the recirculation zones on the left and right sides, respectively. Stable flames at lower equivalence ratios with 10% hydrogen content, Figure 23, were smaller becoming more stretched for the 20% hydrogen content mixture, Figure 24. For both conditions the increase of equivalence ratio resulted in increasingly stretched recirculation zones, Figures 23d and 24d. Once the equivalence ratio exceeded a critical value, the flame propagated upstream distorting these zones; the complete flame flashback condition can be seen in Figures 23f and 24f. Figures 23f and 24f revealed that during flashback, the 20%H_2+80%CO blended flames possessed higher backward velocity momentum compared to the 10%H_2+90%CO flames. The percentage of H_2 dictated the intensity of flashback due to its high thermal and mass diffusivities creating a complex vortex-chemistry interaction

inside the combustor. Flames with higher concentrations of H_2 saw the recirculation zones breakdown sooner resulting in higher propensity for flame flashback.

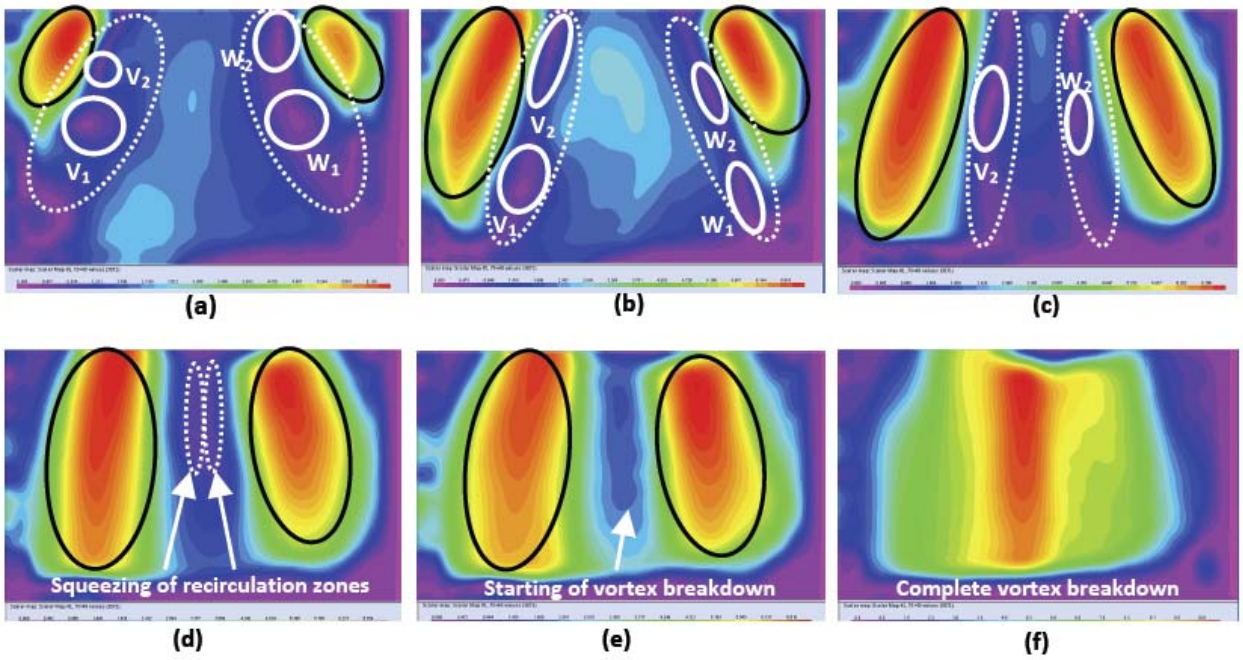

Figure 23: Sequence of a CIVB flashback for a fuel mixture of 10% H_2 and 90% CO with S = 0.97; areas enclosed by solid black, dotted white, and solid white lines represent the approximate location of flames, recirculation zones, and vortices, respectively

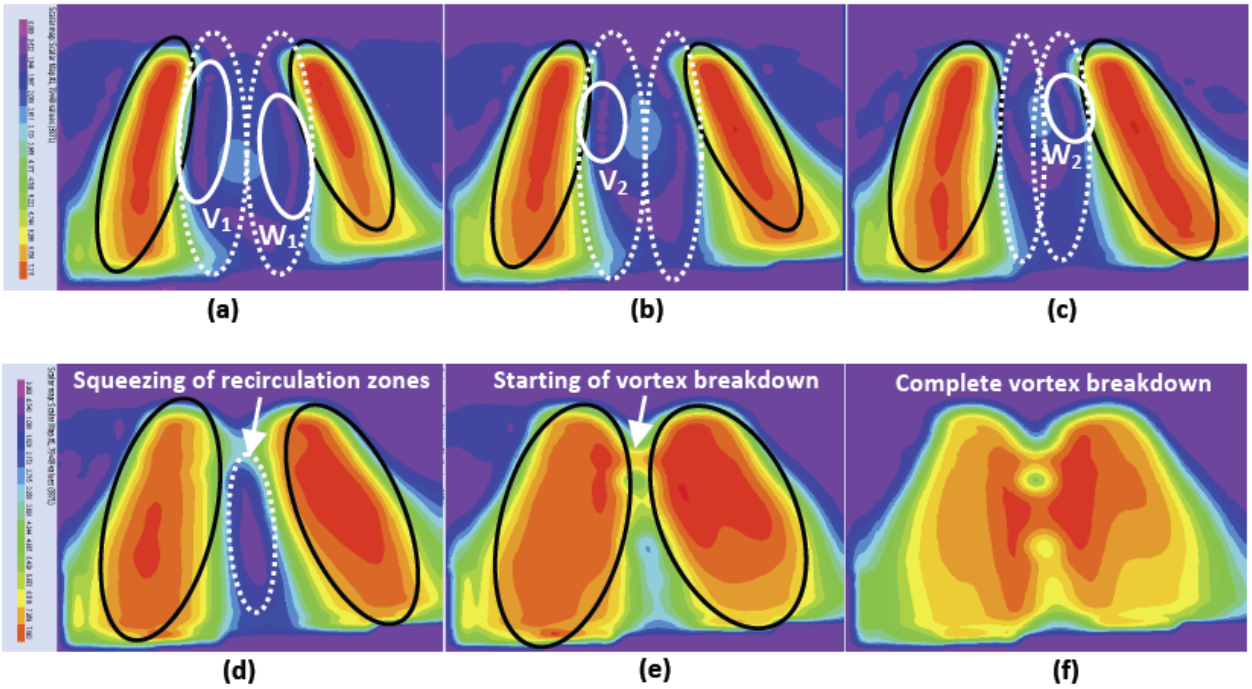

Figure 24: Sequence of a CIVB flashback for a fuel mixture of 20% H_2 and 80% CO with S = 0.97; areas enclosed by solid black, dotted white, and solid white lines represent the approximate location of flames, recirculation zones, and vortices, respectively.

Figures 20, 23, and 24 present the flow visualization of a typical flashback sequence for the same Swirl number S = 0.97 of CH_4 and H_2-CO fuel blends, respectively. A comparison of Figure 20a with Figures 23a and 24a revealed that the H_2-CO-air flow field had a wider recirculation zone. Hence, the pressure gradient inside the flame due to hot gas expansion was more significant in the case of H_2-CO flame. Although flashback occurred at leaner conditions for flames with hydrogen, the sequence of flame flashback behavior was observed to be similar for both CH_4 and H_2-CO fuel blends. In both cases, the swirler generated stable flames close to two side-walls of the combustion chamber at a low equivalence ratio allowing sufficient space for the formation of recirculation zones. As the equivalence ratio increased, the balance between the recirculation tip and flame tip was disturbed eventually resulting in the breakdown of the recirculation zones and flashback.

Effect of Swirl Strength

To investigate the effect of swirl strength, flashback limit data were re-plotted for the two different-strength swirlers. Figure 25 shows the flashback limits for 10%H_2+90%CO and air mixture flame with S = 0.97 and 0.71. From Figure 25 it can be seen that the 6-vane swirler (S = 0.71) was more prone to CIVB flashback compared to the 12-vane swirler (S = 0.97). Therefore, for a given air mass flow rate the tendency of CIVB flashback of a swirl combustor decreased with increased swirl strength. The flow visualization of the flashback sequence for 10%H_2+90%CO fuel blend with S = 0.97 was already presented in Figure 23. Figure 26 presents a sample flow visualization of the flashback sequence for the same fuel composition but with a lower swirl strength, S = 0.71. A comparison of the flow visualization images presented in Figs. 23 and 26 show that the higher strength swirler produces a more intense and well-defined recirculation zone in front of the swirler tip. This allows the generation of a more stable flow field decreasing the flashback propensity of the fuel mixture.

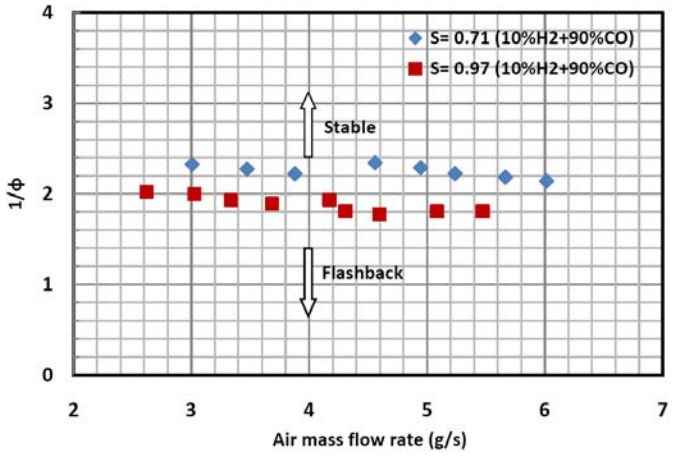

Figure 25: Flashback limits for 10%H_2+90%CO blend mixture with S = 0.97 and S = 0.71

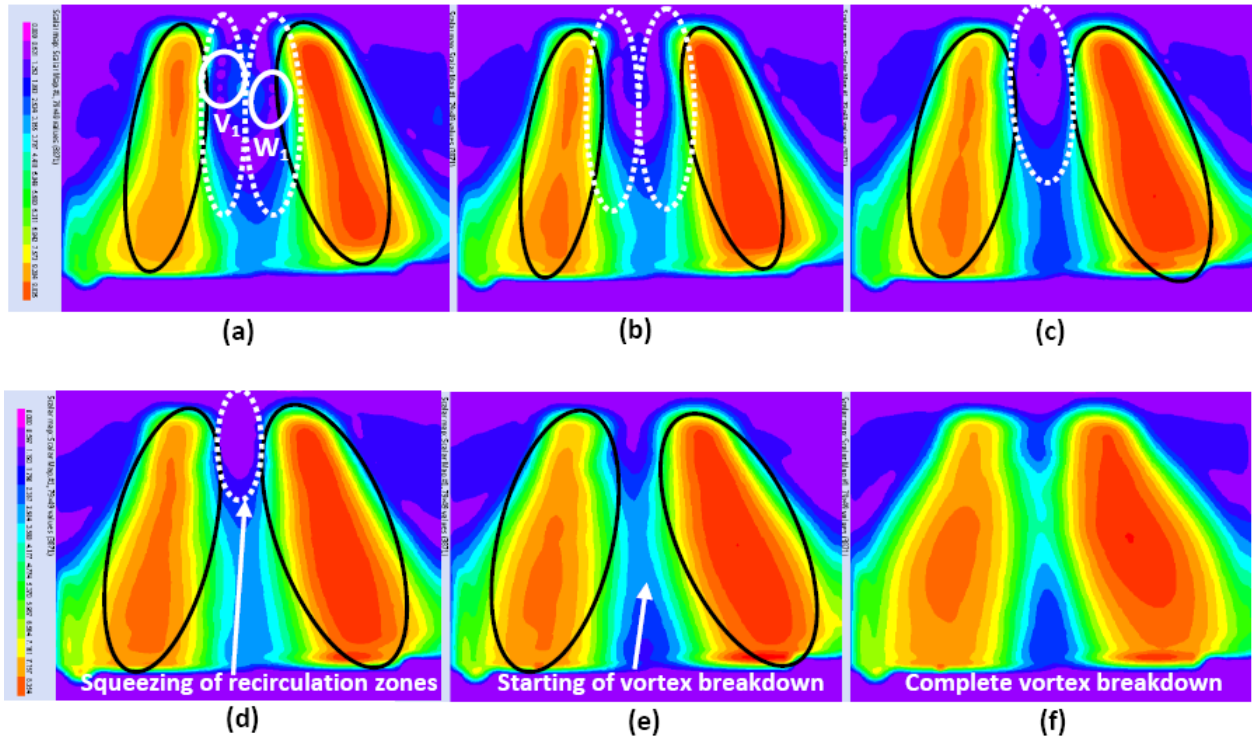

Figure 26: Sequence of a CIVB flashback for a fuel mixture of 10% H_2 and 90% CO with S = 0.71; areas enclosed by solid black, dotted white, and solid white lines represent the approximate location of flames, recirculation zones, and vortices, respectively

Effect of Fuel Concentration in Actual Syngas Mixtures

Hydrogen and carbon monoxide are the two major constituents of syngas fuels, although significant amounts of N_2, CO_2, CH_4, and higher hydrocarbons are also present in the fuel mixture depending on the feedstock and gasification methods. To produce combinations of actual syngas fuels H_2, CO, N_2, CO_2, and CH_4 were mixed according to their percentages as indicated in Table 3.

Table 3: Composition of different synthesized gases Ref. [28]

Gasification	Types of coal	CO (%)	H_2 (%)	CH_4 (%)	N_2 (%)	CO_2 (%)	Calorific Value (MJ/m^3)
Coal	Brown Coal	16	25	5	40	14	6.28
	Bituminous	17.2	24.8	4.1	42.7	11	6.13
	Lignite	22	12	1	55	10	4.13
	Coke	29	15	3	50	3	6.08
Wood		2.1	21	1.83	43	12	7.07

CIVB flashback limits measured for four different syngas compositions with S = 0.97 are shown in Figure 27. The flashback data plotted in this graph follows a similar pattern to those observed by H_2-CO fuel blends. For a given air mass flow rate, flashback was primarily dominated by the percentage of H_2 in the blend. The higher the percentage of H_2 in the mixture, the more susceptible to flashback the flame was. Therefore, brown coal and bituminous containing higher percentage of H_2 were more inclined to propagate upstream in comparison to lignite and coke for the same air mass flow rate. It was also observed that brown and bituminous coal which lay on the higher air excess ratio side of Figure 27 contained an approximately equal percentage of H_2. Hence, for a given air mass flow rate their flashback limits were similar. This observation was also true for lignite and coke flames which have comparable percentage of H_2 and produced flashback limit data on the lower air excess ratio portion of the graph,.

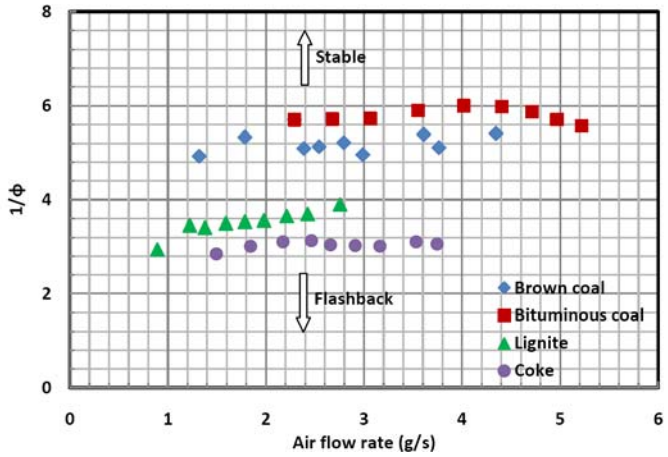

Figure 27: Flashback limits for actual syngas composition with S = 0.97

Of the two major diluents CO_2 and N_2, CO_2 was observed to play a more dominant role in the flame flashback limits. Since brown and bituminous coal possess comparable quantities of H_2 and CO, their flashback limits were similar. The difference between their flashback data was due to the presence of CO_2. The higher percentage of CO_2 in brown coal retards its flashback propensity. CO_2 restricts the active free radicals and increases the recombination reaction rather than chain transfer reaction. Therefore, for a given air mass flow rate brown coal flame undergoes CIVB flashback at a relatively rich condition in comparison to the bituminous flame.

Parametric Modeling

To generalize the measured CIVB flashback limit data for various H_2-CO fuel mixtures, a parametric model similar to Peclet Number (Pe) approach has been developed. For a better representation of the realistic physical processes involved during flashback, the flame quenching concept has been adopted within the model. Previously Peclet Number approach has been effectively used to describe lean-blowout [29] and boundary layer flashback [6] conditions. This model assumes that the controlling parameters (fuel type, equivalence ratio, flow velocity, and burner geometry) for both blowout and flashback were essentially the same. According to Li and

Gutmark [30] and Putnam and Jensen [31], the flow Peclet Number varies with square of the flame Peclet Number. Thus, the parametric relation between these parameters is [4]:

$$\mathbf{Pe_{flow} \propto Pe_{flame}^2} \tag{26}$$

with $\mathrm{Pe_{flow}(or\ Pe_U)} = \dfrac{UD}{\alpha}$ and $\mathrm{Pe_{flame}(or\ Pe_{SL})} = \dfrac{S_L D}{\alpha}$, where U is the characteristic velocity (bulk velocity in the present case), D is the characteristic dimension (diameter of the mixing tube is the present case), S_L is the flame propagation velocity, and α is the thermal diffusivity of the mixture. Eq (26) can be modified by introducing an experimental constant:

$$\mathbf{\frac{UD}{\alpha} = C\frac{S_L^2 D^2}{\alpha^2}} \tag{27}$$

Kröner et al. [4] termed constant C as a quench parameter C_{quench} which represents a quality factor for specific burner design. Thus, a quench factor C_{quench} can be easily translated into a Peclet Number model for flame quenching as in the case of present investigation.

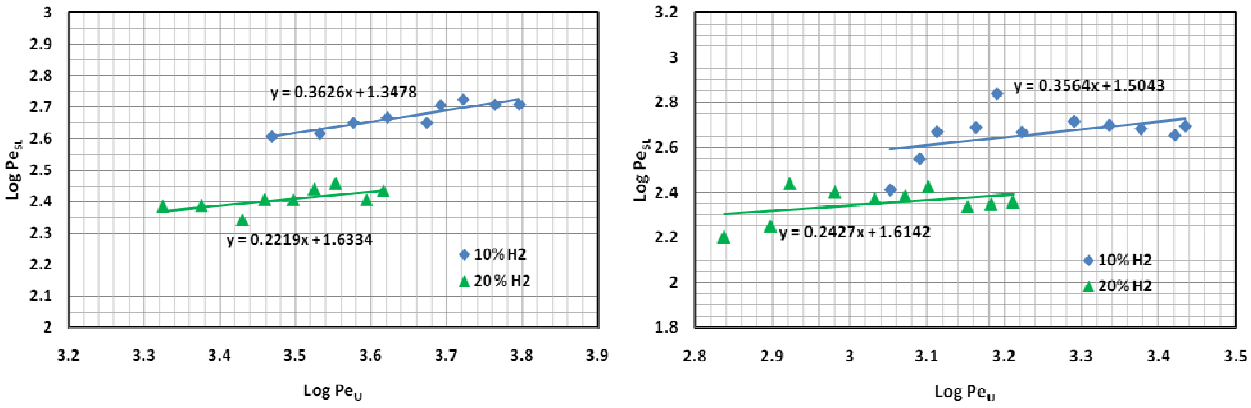

(a) (b)

Figure 28: Correlation of flame quenching at the flashback limit based on Peclet Numbers for fuel mixtures of 10%H2+90%CO and 20%H2+ 80%CO with: (a) 12 vane swirler (S = 0.97), (b) 6 vane swirler (S = 0.71)

Figure 28 presents a correlation between the flow Peclet Number Pe_U and the flame Peclet Number Pe_{SL} with 10%H_2+90%CO and 20%H_2+80%CO fuel mixtures at S = 0.97 (Figure 28a) and S = 0.71 (Figure 28b). The correlation between the Peclet Numbers are re-plotted for two Swirl Numbers in Figure 29 with 29a representing that for 10%H_2+90%CO fuel mixture and 29b or a 20%H_2+80%CO mixture. To calculate Peclet Numbers, the flame velocity data and S for different fuel compositions has been experimentally generated [31] and the thermal diffusivity α for various air-fuel mixtures was evaluated using CHEMKIN software. It is evident from Figure 28 that at both S = 0.97 and 0.71 the fuel containing lower percentage of H_2 yields the higher quench factor. Since the 12 vane swirler generated a more stable flame and well-defined recirculation zones, the data in Fig 15a showed less scattering than that in Figure 28b. It can also be seen from Figure 29 that both swirlers yield the same value of C_{quench} for similar fuel compositions. For the 10%H_2+90%CO fuel composition the value of C_{quench} was found

approximately 0.36 (Figure 29a) and for the 20%H_2+80%CO fuel composition the value was approximately 0.23 (Figure 29b). Therefore, C_{quench} was dominated mostly by the fuel composition rather than the swirl strength.

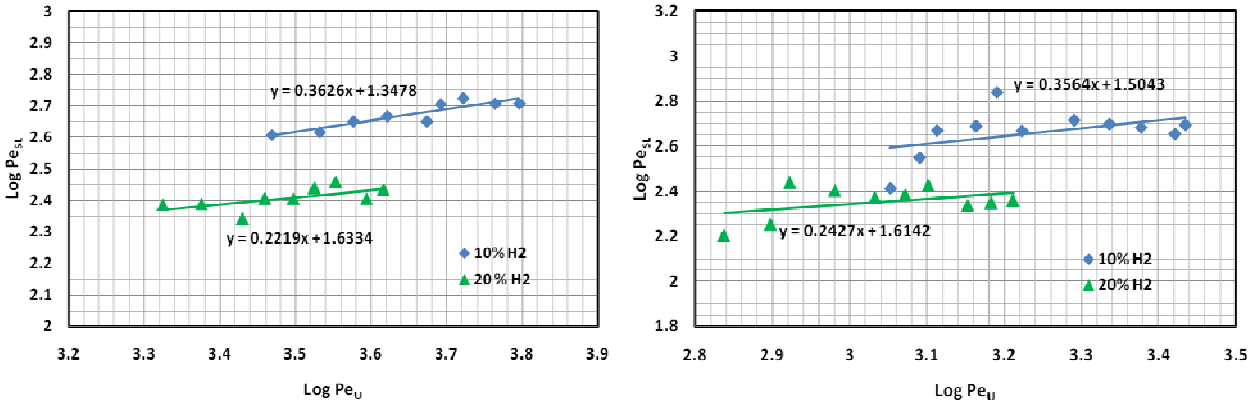

(a) (b)

Figure 29: Correlation of flame quenching at the flashback limit based on Peclet Numbers for fuel mixtures of: (a) 10%H_2+90%CO, (b) 20%H_2+80%CO.

IV. c Preliminary Numerical Results

For the two combustion models investigated a perfectly premixed mixture of methane-air with an equivalence ratio of 0.77 was injected into the combustion chamber initially held at ambient conditions (1 atm, 298K). The mixture was then ignited upstream of the swirler. The reaction zone was then observed to propagate upstream and stabilize on the centerbody of the swirler. A sample of the results showing the velocity and temperature contours of the reaction zone at some point in the simulation for the species transport model are shown in Figure 30 and Figure 31. Figures 30 and 31 show the cross-sectional view of the combustion chamber; this view allows for a detailed study of the formation of eddies and mixing characteristics occurring within the chamber.

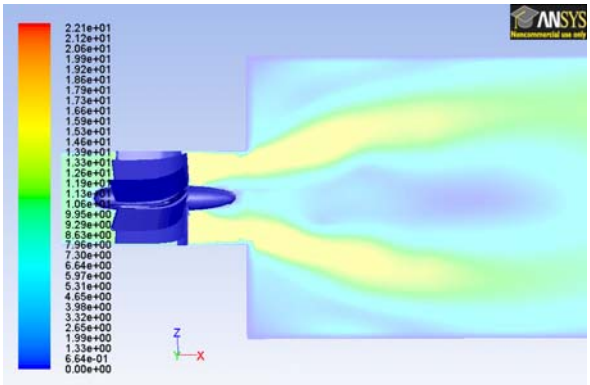

Figure 30: Velocity profile for the species transport combustion model

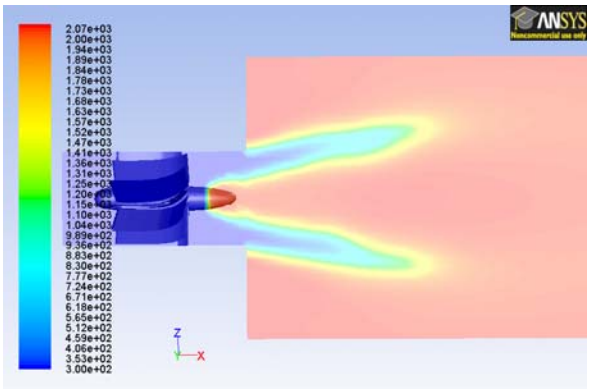

Figure 31: Temperature profile for the species transport combustion model

The same methodology was followed for the XiFoam combustion model; the premixed fuel was injected at the inlet, and the mixture was then ignited upstream of the swirler. Figure 32 shows the flame front propagating upstream after being ignited at t=0.

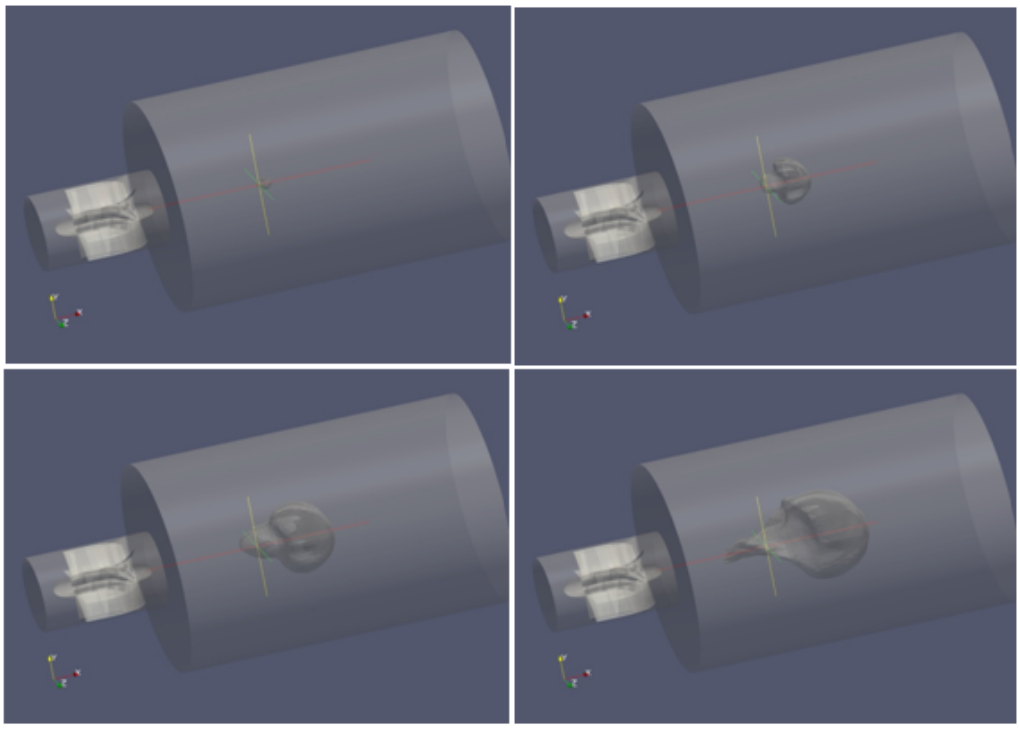

Figure 32: Flame propagation after ignition using XiFoam combustion solver with a d*t* = 0.01s

V. Conclusions

For the first part of the experimental testing it was observed that the boundary layer flashback propensity of H_2-CO and H_2-CH_4 flames changes nonlinearly with the increase in H_2 contents in the mixture. Also, for H_2-CO flames g_F values increase abruptly with the increase in H_2 concentration in fuel rich mixtures. For H_2-CH_4 flames g_F values increase with an increase in H_2 concentration for fuel lean mixtures, an increase of H_2 in the mixture for fuel mixtures above 9% concentration did not significantly affect the critical boundary velocity gradient. The increase in g_F value with H_2 concentration in N_2 diluted mixtures is not limited to rich conditions.

For the second part of the experimental investigation, the CIVB flashback limit was carried out for H_2-CO fuel blends and actual syngas fuel compositions. The effects of different constituent concentrations and Swirl number on flashback propensity were discussed. The study revealed that CIVB flashback propensity was mostly dominated by H_2 concentration in the fuel mixtures. For a given air mass flow rate, the mixture containing higher H_2 concentration underwent flashback at leaner conditions. Combustion of actual syngas fuel compositions showed that CO_2 was found to be more dominant than N_2. It was also shown that for a given air mass flow rate flashback propensity of a swirl combustor decreased with increased swirl strength. To probe the magnitude of fuel composition and swirler strength, a parametric model similar to Peclet Number approach was developed employing flame quenching concept. Using a correlation between flow Peclet Number and flame Peclet Number a quench parameter, C_{quench}, was introduced which was observed to be dominated by the fuel composition rather than swirl strength.

The third section of this report used both commercial code (CHEMKIN CFD) and open source codes (OpenFOAM) to numerically investigate the flashback process occurring in the combustor used for the experimental portion of this work. An LES model was developed for both isothermal and reacting flow, future work is planned for this topic looks to continue as future planned work.

The information gained from the project contributes to the improvement of understanding of flashback due to both boundary layer and in particular CIVB. Data here will contribute to developing design tools for fuel flexible turbine combustors and allow for the determination of design margins against flashback under CIVB.

VI. References

[1] Turbine Technologies Website, National Energy Technology Laboratory, Department of Energy, Web Address: http://www.netl.doe.gov/technologies/coalpower/turbines/index.html

[2] Fick, W., Griffiths, A. J., and O'Doherty, T., 1997, "Visualization of the Precessing Vortex Core in an Unconfined Swirling Flow, Optical Diagnostics in Engineering," **2(1)**, pp. 19-31.

[3] Fritz, J., Kroner, M., and Sattelmayer, T., 2004, "Flashback in a Swirl Burner with Cylindrical Premixing Zone," ASME Journal of Engineering for Gas Turbines and Power, **126**, pp. 276-283.

[4] Kröner, M., Fritz, J., and Sattelmayer, T., 2003, "Flashback Limits for Combustion Induced Vortex Breakdown in a Swirl Burner," ASME Journal of Engineering for Gas Turbines and Power, **125**, pp. 693-700.

[5] Kiesewetter, F., Kirsch, C., Fritz, J., Kroner, M., and Sattelmayer, T., 2003, "Two-Dimensional Flashback Simulation in Strongly Swirling Flows," Proceedings of ASME Turbo Expo, June 16-19, 2003.

[6] Lewis, B., and von Elbe, G., 1987, Combustion, Flames, and Explosion of Gases, 3rd edition, Academic Press, Orlando.

[7] Davu, D., Franco, R., Choudhuri, A., and Lewis, R., 2005, "Investigation on Flashback Propensity of Syngas Premixed Flames," AIAA Paper No. 2005-3585.

[8] Choudhuri, A. R., 2005, "Investigation of the Effects of Composition and Combustion Instabilities on the Flashback Propensity of Syngas Premixed Flames," Final Technical Report, Department of Energy Grant DE-FG26-04NT42133.

[9] Sommerer, Y., *Galley, D., Poinsot, T., Ducruix, S., Lacas, F., and Veynante, D.,* 2004, "Large Eddy Simulation in a Lean Partially Premixed Swirled Burner, Journal of Turbulence," **5**, pp. 37-37(1).

[10] Wegner, B., Kempf, A., Schneider, C., Sadiki, A., and Schafer, M., 2004, "Large Eddy Simulation of Combustion Processes under Gas Turbine Conditions," Prog. Computational Fluid Dynamics. **4**, pp**.** 257–63.

[11] Weller , H. G., Tabor , G., Gosman , A. D., and Fureby, C., 1998, "Application of a Flame-Wrinkling LES Combustion Model to a Turbulent Mixing Layer," Processing of 27th Symposium (International) on Combustion, pp. 899-907.

[12] Fureby C., and Möller S. I., 1995, "Large eddy simulations of reacting flows applied to bluff body stabilized flames," AIAA J. **33**, pp. 2339-2347.

[13] Thibaut, D., and Candel, S., 1998, "Numerical Study of Unsteady Turbulent Premixed Combustion: Application to Flashback Simulation," Combustion and Flame, **113**, No. 1-2, pp. 53-65.

[14] Wu, X., 2005, "Asymptotic Approach to Combustion Instability," Philosophical Transactions of the Royal Society A, **363**, pp. 1247-1259.

[15] Hathout, J.P., Fleifil, M., Annaswamy, A. M., and Ghoniem, A. F., 2000, "Active Control Using Fuel-injection of Time-delay Induced Combustion Instability," AIAA Journal of Propulsion and Power, **18(2)**, pp.390 -399.

[16] Coats, C. M., 1980, "Comment on Review of Flashback Reported In Prevaporizing/ Premixing Combustors," Combustion and Flame, **37**, pp. 331-333.

[17] Joos. F., and Vortmeyer D., 1986, "Self-Excited Oscillations in Combustion Chambers with Premixed Flames and Several Frequencies," Combustion and Flame, **65**, pp. 253-262.

[18] Schimmer, H., and Vortmeyer, D., 1977, "Acoustical Oscillation in a Combustion System with a Flat Flame," Combustion and Flame, **28**, pp. 17-24

[19] Fleifil, M., Annaswamy, A. M., Ghoneim Z. A., and Ghoniem A. F., 1996, "Response of a Laminar Premixed Flame to Flow Oscillations: a Kinematic Model and Thermoacoustic Instability Results," Combustion and Flame, **106**, pp. 87-510.

[20] Gupta, A. K., and Lilley, D. G., 1985, Swirl Flows, Abacus press, Cambridge, Massachusetts, USA.

[21] Leibovich, S., 1978, "The Structure of Vortex Breakdown," Annual Review of Fluid Mechanics, **10**, pp. 221–246.

[22] Choudhuri A., Subramanya, M, and Gollahalli, S. R., 2008, "Flame Extinction Limits in Fuel Blends," Journal of Engineering for Gas Turbine and Power, **130**, Issue 3, 031501.

[23] Noble D. R., Zhang, Q., Shareef, A., Tootle, J., Meyers, A., and Lieuwen, T., 2006, "Syngas Mixture Composition Effects upon Flashback and Blowout," ASME Paper No. GT-2006-90470.

[24] FLUENT Version 12.0 Theory Guide, April 2009, Fluent Inc

[25] A. Kazakov and M. Frenklach, URL: http://www.me.berkeley.edu/drm/ [Cited May 30, 2011]

[26] Kido HN. Influence of Local Flame Displacement Velocity on Turbulent Burning Velocity. Proceedings of the Combustion Institute, Combustion institute. PA:2002; 20, pp. 1855–1861.

[27] Kido HN. Turbulent burning velocities of two component fuel mixtures of methane, propane and hydrogen. Jpn Soc Mech Eng Int J 2002;45:355–62.

[28] Chomiak, J., Longwell, J. P., and Sarofim, 1989, "Combustion of Low Calorific Value Gases: Problems and Prospects," Prog. Energy Combust. Sci, **15**, pp. 109-129.

[29] Strakey, P., Sidwell, T., Ontko, J., 2007, "Investigation of the effects of Hydrogen Addition of Lean Extinction in a Swirl Stabilized Combustor," Proceedings of the Combustion Institute, **31**, pp. 3173-3180.

[30] Li, G. and Gutmark, E., "Experimental Study of Large Coherent Structure in a Swirl-Dump Combustor," 2004, AIAA Paper 2004-0133.

[31] Putnam, A. A., and Jensen R. A., 1949, "Application of Dimensionless Numbers to Flash-Back and Other Combustion Phenomena," Third Symposium on Combustion and Flame and Explosion Phenomena, Williams and Wilkins, Baltimore, pp.89–98.

VII. List of Symbols, Acronyms and Abbreviations

English

b	=	mean reaction regress variable
c	=	mean reaction progress variable
C_{quench}	=	quenching parameter
C_s	=	Smagorinsky constant
C_ξ	=	volume fraction constant
C_τ	=	time scale constant
d	=	distance closest to the wall in the mixing length formula
D	=	diffusion coefficient
$D_{i,m}$	=	mass diffusion coefficient for species i in the mixture
$D_{T,i}$	=	thermal diffusion coefficient for species i
D_t	=	turbulent diffusivity
$G(x, x')$	=	filtering function
g	=	velocity gradient
g_f	=	critical velocity gradient
J_i	=	diffusion of species i
L_s	=	mixing length for the subgrid scales
p	=	pressure
Pe	=	Peclet Number
Pe_{flame}	=	flame Peclet Number
Pe_{flow}	=	flow Peclet Number
Pe_{SL}	=	flame Peclet Number
Pe_U	=	flow Peclet Number
R_i	=	net rate of production of species i by chemical reaction
S_i	=	rate of creation of species i
S_{ij}	=	mean rate-of-strain tensor
$\bar{S}_{ij}$	=	rate-of-strain tensor for the resolved scales
S_L	=	flame propagation velocity
Sc_t	=	turbulent Schmidt number
S_u	=	laminar flame speed
T	=	temperature
T_b	=	temperature of burnt gases
T_f	=	temperature of unburnt gases
U	=	bulk velocity
Y_i	=	mass fraction of species i
Y_i^*	=	fine-scale species mass fraction

Greek

α	=	thermal diffusivity
Δ	=	local grid scale
δ_{ij}	=	kronecker delta
ε	=	turbulent dissipation rate
ϕ	=	equivalence ratio
k	=	kinetic energy
κ	=	von Kármán constant
μ_t	=	turbulent viscosity
μ	=	dynamic viscosity
ν	=	kinematic viscosity
$\overline{\phi}(x)$	=	filtered variable
ρ	=	density
σ_{ij}	=	stress tensor
τ^*	=	time scale
τ_{ij}	=	subgrid-scale stress
$\vec{u}$	=	velocity vector
Ξ	=	flame wrinkling
ξ^*	=	length fraction of the fine scales